Available online at www.sciencedirect.com
SCIENCE DIRECT
International Journal of Pharmaceutics 307 (2006) 103–113
international journal of pharmaceutics
www.elsevier.com/locate/ijpharm

Pharmaceutical Nanotechnology

Nanoparticle formulation may affect the stabilization of an antiischemic prodrug

E. Leo [a], C. Contado [b], F. Bortolotti [c], B. Pavan [d], A. Scatturin [c], G. Tosi [a], S. Manfredini [c], A. Angusti [c,1], A. Dalpiaz [c,*]

[a] *Dipartimento di Scienze Farmaceutiche, Modena and Reggio Emilia University, via G. Campi 183, I-41100 Modena, Italy*
[b] *Dipartimento di Chimica, Ferrara University, via Borsari 46, I-44100 Ferrara, Italy*
[c] *Dipartimento di Scienze Farmaceutiche, Ferrara University, via Fossato di Mortara 19, I-44100 Ferrara, Italy*
[d] *Dipartimento di Biologia, Sezione di Fisiologia Generale, Ferrara University, via Borsari 46, I-44100 Ferrara, Italy*

Received 11 May 2005; received in revised form 22 September 2005; accepted 29 September 2005
Available online 14 November 2005

Abstract

The prodrug 5′-octanoyl-CPA (Oct-CPA) of the antiischemic N^6-cyclopentyladenosine (CPA) has been encapsulated by nanoprecipitation in poly(lactic acid) nanoparticles, which have been recovered by gel-filtration, ultra-centrifugation or dialysis. We have analysed how different surfactants and purification methods can influence the nanoparticle characteristics. The particle sizes have been obtained by scanning electron microscope, whereas a SdFFF system was employed to detect their distributions. The Oct-CPA release from nanoparticles and stabilities in human blood of free and encapsulated prodrug have been analysed by HPLC techniques. The effects of nanoparticles on CPA interaction toward adenosine A_1 receptor (its action site) have been analysed using radiolabelled drugs. The smallest nanoparticles and the best degree of homogeneity have been obtained using sodium cholate; the best recovery has been achieved by dialysis, whereas gel-filtration and ultra-centrifugation have induced the greatest removal of surfactants. The release of Oct-CPA was better controlled from the nanoparticles obtained using Pluronic F68 and purified by gel-filtration or ultra-centrifugation. Similarly, these nanoparticles better increased the stability of the prodrug in human blood. In particular, the nanoparticles purified by ultra-centrifugation induced a strong stability to a fraction of the encapsulated Oct-CPA. Any interference by unloaded nanoparticles has been registered for CPA-adenosine A_1 receptor interaction.

Keywords: Controlled release; N^6-cyclopentyladenosine; Nanoparticles; Prodrug; SdFFF; Stability

1. Introduction

Adenosine and its N^6-substituted derivatives show a neuroprotective role which has been observed by a great number of studies (Dalpiaz and Manfredini, 2002). The neuroprotective effect is related to the ability of these compounds to activate the adenosine receptor subtype A_1 (Fredholm et al., 1994; Ralevic and Burnstock, 1998), inducing a neuronal membrane hyperpolarisation and a consequent decrease of the release of excitatory amino acids (de Mendonca et al., 2000). The strategic role of A_1 receptors as neuroprotectors is underlined by the results of recent studies, indicating that mice deprived of adenosine A_1 receptors posses a reduced protection against the degenerative effects caused in the brain by hypoxia (Johansson et al., 2001). As a consequence, it is reasonable to hypothesise that ischemia-related structural and functional damages of the central nervous system may be reduced or prevented by the activation of adenosine A_1 receptors in the brain (Bischofberger et al., 1997). In this regard, it has been demonstrated that selective adenosine A_1 agonists allow to protect gerbils from damage to the hippocampus and to increase their survival following ischemic injury (Von Lubitz and Marangos, 1990; Von Lubitz et al., 1999).

Even if laboratory results suggest that A_1 agonists may have promising effects against SNC ischemic damages, these compounds have not entered in the clinical use, because of (i) they can be quickly degraded in blood (Mathot et al., 1994; Pavan and IJzerman, 1998), (ii) they are not able to reach the brain by the systemic way (Brodie et al., 1987) and finally (iii) they cause

* Corresponding author. Tel.: +39 0532 291273; fax: +39 0532 291296.
E-mail address: dla@dns.unife.it (A. Dalpiaz).
[1] Present address: Biotechnology Research Institute (NSERC), Biological Chemistry Department, Montreal, Canada.

0378-5173/$ – see front matter © 2005 Elsevier B.V. All rights reserved.
doi:10.1016/j.ijpharm.2005.09.031

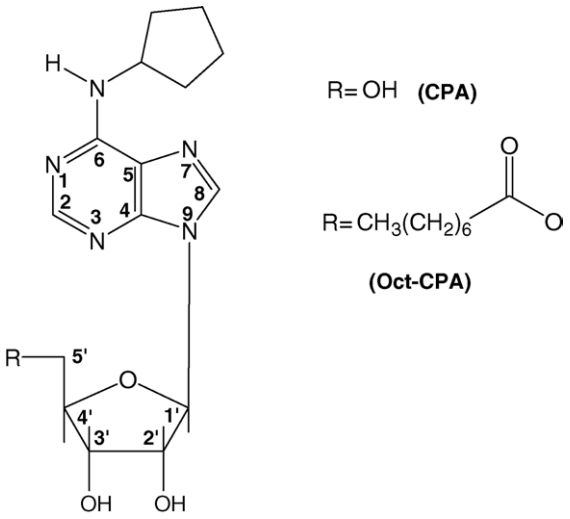

Fig. 1. Chemical formulas of N^6-cyclopentyladenosine (CPA) and its prodrug 5′-octanoyl-CPA (Oct-CPA).

relevant side effects at other organs (Jacobson et al., 1991; Von Lubitz et al., 1999).

In the aim to find a solution for the difficulties above described, we have taken into account the prototypic A_1 receptor agonist N^6-cyclopentyladenosine (CPA, Fig. 1) (Muller, 2000) and we have proposed either a prodrug approach (Dalpiaz et al., 2001a), or preliminary encapsulation studies in micro- and nano-controlled release systems (Dalpiaz et al., 2001b, 2002, 2005). In particular, 5′-esters of CPA were proposed as prodrugs able to increase its stability in blood and diffusion through lipid barriers. Among these, the 5′-octanoyl-CPA (Oct-CPA, Fig. 1) prodrug appears hydrolysed in whole blood only by plasmatic esterases, showing an half life about 30 min (Dalpiaz et al., 2001a). We have, moreover, demonstrated that CPA can be encapsulated in poly(lactid acid) microspheres which allow to obtain its controlled release and a related strong stabilisation in human whole blood (Dalpiaz et al., 2001b, 2002). Our preliminary encapsulation studies of CPA and its prodrug Oct-CPA in biodegradable nanoparticles suggest that the prodrug can be encapsulated more successfully than CPA, and that the controlled release of Oct-CPA allow to obtain a reduction of its hydrolysis rate in human blood (Dalpiaz et al., 2005).

Taking into account that the nanoparticle approach appears a promising strategy in the attempt to enhance the therapeutic effects of drugs potentially active in the brain (Kreuter et al., 1997; Calvo et al., 2002), we report a detailed study in the aim to formulate and characterise Oct-CPA loaded poly(lactic acid) nanoparticles. In particular, we have analysed the effects of the surfactants and the recovery methods on the size of nanoparticles, the prodrug loading, its release modalities and the related stabilisation in whole blood. The morphology of the nanoparticles has been analysed using a scanning electron microscope (SEM), whereas the particle size distribution has been achieved with a chromatography-like elution technique called sedimentation field-flow fractionation (SdFFF), which separates colloids and particles on the basis of differences in effective mass (Kirkland et al., 1980; Caldwell and Li, 1989; Giddings, 1993, 1995; Giddings and Williarns, 1993; Giddings and Ho, 1995; Contado et al., 1997).

The effects of nanoparticles on the target site of CPA, i.e. the human adenosine A_1 receptor, have been finally investigated.

2. Materials and methods

2.1. Materials

[^{3}H]1,3-dipropyl-8-cyclopentylxanthine ([^{3}H]DPCPX, 108 Ci/mmol) was obtained from NEN Research Products (Boston, MA, USA). CPA, N^6-cyclohexyladenosine (CHA), adenosine deaminase (ADA), sulphosalicilic acid, polyethylene–polypropylene glycols (Pluronic F-68), sodium cholate were obtained from Sigma (St. Louis, MO, USA). The prodrugs Oct-CPA and 5′-cyclohexanoyl-CPA (CH-CPA) were synthesised as previously described (Dalpiaz et al., 2001a). CHO cells transfected with adenosine A_1 human receptors were a kind gift of Prof. Peter R. Schofield (Garvan Institute of Medical Research, Darlinghurst, Australia) (Townsend-Nicholson and Shine, 1992; Townsend-Nicholson and Schofield, 1994). Foetal bovine serum (FBS), 1:1 mixture of Dulbecco's modified Eagle's medium and Ham's F12 medium, streptomycin and penicillin, trypsin-EDTA and phosphate buffered saline (PBS) were obtained from Invitrogen (Life Technologies Italia, Milan, Italy). HPLC grade solvents were purchased from Carlo Erba Reagenti (Milan, Italy). Poly(D,L lactic acid) (PLA, mean molecular weight 16,000; Resomer® R203; Boehringer-Ingelheim, Ingelheim am Rhein, Germany) was utilised as biodegradable polymer to prepare the nanoparticles. All other chemicals and solvents were obtained from standard sources.

2.2. Nanoparticle preparation

Nanoparticles were prepared according to the nanoprecipitation method (Fessi et al., 1989). Practically, accurately weighed amount PLA polymer (125 mg) was dissolved in acetone (4 ml) and the prodrug Oct-CPA (2 mg) was dissolved in methyl alcohol (8 ml). The organic phase (acetone + methyl alcohol) was added dropwise into the 25 ml deionised water (aqueous phase) containing Pluronic F-68 or sodium cholate (125 mg). After stirring magnetically at room temperature for 15 min, the organic solvent was removed at 35 °C using a Rotavapor (Mod. B-480, Büchi Labortechnik, Flawil, Switzerland) under vacuum (about 30 mmHg). The final volume of the suspension was adjusted to 10 ml with deionised water before nanoparticle recovery.

Empty nanoparticles were prepared according the procedure previously described, omitting obviously the drug. The nanoparticles were purified by dialysis technique (T3, Cellusep, Seguin, TX, USA), by gel-filtration chromatography (Sepharose CL4B; Sigma Chemical) or by ultra-centrifugation (Sorvall® RC28S, DuPont, Willmington, DE, USA).

Dialysis technique was carried out introducing the colloidal supension containing the nanoparticles (10 ml) in a dialysis tube (exposed surface 5 cm) hermetically sealed (i.d. 18 mm; MWCO 12000, T3, Cellusep, Seguin, TX, USA) and dialyzing at 37 °C against 500 ml of deionised water for 2 h under magnetic stirring.

Gel-filtration chromatography was carried out using a Sepharose CL4B (Sigma Chemical) gel. The gel was filled into a column, avoiding bubbles and cracks. The column had a length of 50 cm, an inner diameter of 2 cm and contained about 160 ml of gel. The nanoparticles were eluted using deionised water at a flow rate adjusted to 1.5 ml/min. The appearance of the nanoparticles in the eluate was pointed out in about 20 min using a turbidimeter (model DRT 15-CE, HF Scientific Inc., Fort Meyers, FL, USA).

The nanoparticle purification by ultra-centrifugation was performed at 10,000 × *g* for 10 min using a F38/36 rotor (DuPont). The nanoparticles were treated three times, each time using 2 ml of deionised water.

The samples collected were freeze-dried during 24 h (Lyovac GT2; Leybold-Heraeus, Hanau, Germany) to obtain a fine powder of nanoparticles. All samples were prepared a purified in triplicate. The yield of nanoparticles was calculated as the ratio of the amount of recovered nanoparticles to the total amount of polymer and drug added.

2.3. Particle size measurement and morphological analysis

A scanning electron microscope (SEM) (XL-40 Philips, The Netherlands) was used to evaluate both size and morphology of nanoparticles. The samples were mounted on aluminium stubs (TAAB Laboratories Equipment, Berks, UK) using double-sides sticky tape (TAAB laboratories Equipment). Before the SEM analysis, the samples were coated under argon atmosphere with a 10-nm gold palladium thickness (Emitech K550 Supper Coated, Emitech LTD, Ashford, Kent, UK).

A SdFFF system (Model S101, FFFractionation, Inc., Salt Lake City, UT), with hastelloy C channel walls, was empoyed to determine the size distribution of the particles. Nominal channel dimensions, cut from a mylar spacer, were 90 cm (tip-to-tip length), 2 cm (breadth) and 0.0254 cm (thickness); the void volume of 4.86 ml was empirically determined from injections of rapidly diffusing low molecular weight solutes, e.g. sodium benzoate.

An HPLC Pump model 422 Master (Kontron Instruments, Italy) was used to deliver the carrier. The outlet tube from the channel was connected to a UV detector operating at 240 nm (Uvidec 100, Jasco Ltd., Japan). The signal $c(t_r)$ was collected by an ACRO-900 12 bit I/O acquisition system (Acrosystems Co. Beverly, MA, USA), stored and elaborated with a PC-compatible computer.

The mobile phase was a 0.01% (w/v) solution of polyvinyl alcohol 8–88 (81383 Fluka Chemie GmbH, Buchs, Switzerland) in Milli-Q water (Millipore S.p.A., Vimodrone, Milan, Italy), flowing at 2 ml/min.

The samples were injected with a Hamilton syringe directly into the channel; the injected volume was 100 μl of 0.1% (w/v) suspension.

The fractograms, i.e. the graphical results, have been converted in particle size distribution (PSD) knowing the particle density. In order to achieve the mean size and the correspondent standard deviation of the main peaks, the PSDs plot were then deconvoluted with Peakfit-v4 (Jandel, Scientific Software) by using the Exponentially Modified Gaussian function, and the residual method.

2.4. Oct-CPA content in the nanoparticles

To evaluate the prodrug content in nanoparticles, an accurately weighted amount of nanoparticles (about 5 mg) were used to obtain a suspension in water (1 ml). Five hundred microlitres of water and 200 μl of dichloromethane were added to 100 μl of suspension. Five hundred microlitres of 10% sulphosalicilic acid and 50 μl of 30 μM CH-CPA (as internal standard) were used for Oct-CPA extraction. The samples were extracted twice with 900 μl of water saturated ethylacetate. After 5 min of centrifugation at 9000 × *g*, the organic layer was evaporated to dryness by N_2 flow; 200 μl of mobile phase (see below) were added and after centrifugation, 20 μl were injected into the HPLC system for the content analysis.

Prodrug loading and entrapment efficiency were calculated according to the following equations:

$$\text{prodrug loading (\%, w/w)} = \frac{\text{mass of prodrug in nanoparticles}}{\text{mass of nanoparticles recovered}} \times 100 \quad (1)$$

$$\text{entrapment efficiency (\%)} = \frac{\text{mass of prodrug in nanoparticles}}{\text{starting mass of prodrug}} \times 100 \quad (2)$$

2.5. HPLC analysis of Oct-CPA

The HPLC apparatus consisted of a modular chromatographic system (model 1100 series pump and diode array detector; Agilent, Waldbroon, Germany) linked to an injection valve with 50 μl sample loop (model 9125; Rheodyne, Cotati, CA, USA). The detector was set at 269 nm. Chromatography was performed at room temperature on a reverse-phase column (Hypersil BDS C-18 5U cartridge column, 150 mm × 4.6 mm i.d.; Alltech Italia Srl BV, Milan, Italy) equipped with a guard column packed with Hypersil C-18 material (Alltech). Data acquisition and processing were accomplished with a personal computer using Chem Station software (Agilent). The mobile phase consisted of a ternary mixture of acetonitrile, methanol and 10 mM acetate buffer (pH 4) with a ratio of 4/54/42. The flow rate was 0.8 ml/min and retention times were 7.7 and 3.9 min for Oct-CPA and CH-CPA, respectively.

2.6. Determination of Pluronic F68 residuals

The amount of Pluronic F68 associated with nanoparticles was determined by a colorimetric method based on the formation of a colored complex between two hydroxyl groups of Pluronic F68, Ba^{2+} and an iodine molecule (Childs, 1975). Briefly, 10 mg of lyophilised nanoparticles was dissolved in 2 ml of dichloromethane. Then, 10 ml of deionised water were added and stirred until complete evaporation of the solvent (2 h). After the centrifugation of the water phase at 4200 rpm for

10 min (model 4235, A.L.C., Milan, Italy), 1 ml of a 5% (w/v) $BaCl_2$ solution in HCl 0.1 M and 1 ml of a solution of I_2/KI (0.05 M/0.15 M) were added to 4 ml of supernatant. Finally, the absorbance of the samples was measured spectophotometrically at 540 nm (WPA lighwave, Cambridge, UK) after 15 min incubation at room temperature. No absorption was observed when only PLA polymer was used under identical condition.

2.7. Determination of sodium cholate residual

An accurately weighed amount of nanoparticles (10 mg) was dissolved in 2 ml of dichloromethane. After the complete nanoparticles dissolution, deionised water (5 ml) was added to extract sodium cholate. The bile salt amount was assayed in the in the filtered solution by an HPLC procedure (Mucci et al., 1996). The analyses were carried out using a Varian 9012 liquid chromatograph (Walnut Creek, CA, USA) equipped with a Jasco UV-1575 detector (Tokyo, Japan) and interfaced to Star Chromatographic Workstation (Varian) software. For the analyses a reversed-phase C_{18} column (Lichrospher 100 RP 18 column; 240 mm × 4.6 mm i.d.; 5 μm particle size; Merck, Darmstadt, Germany) was used. The mobile phase was composed of methyl alcohol–0.02 M sodium acetate buffer in water (80:20, w/w) adjusted to pH 4.3 with phosphoric acid. Twenty microlitres volumes were eluted isocratically (flow rate of 1 ml/min), setting the UV detector at 318 nm.

2.8. In vitro Oct-CPA release studies

Drug release from the nanoparticles was performed at 37 ± 0.2 °C in 0.1 M phosphate buffer, pH 7.4 using perfect sink conditions. In particular, an accurately weighted amount of nanoparticles was suspended in about 20 ml of buffer, in manner to obtain a total amount of Oct-CPA corresponding to 10 μg/ml (<10% saturability values of these compounds). The suspension was maintained stirred magnetically during the release experiment. Aliquots of suspension (150 μl) were withdrawn at fixed time intervals, filtered upon centrifugation at 13,000 × *g* using microcon filter devices (YM 30, Millipore Corporation, Bedford, MA, USA). The filtered solution (40 μl) was injected into the HPLC apparatus for the evaluation of Oct-CPA contents.

The quantitative interpretation of release rate was evaluated using the dissolution time (T_d) (Langenbucher, 1972).

2.9. Kinetic experiments in human whole blood

The stability of Oct-CPA encapsulated in nanoparticles and of free Oct-CPA in the absence and in the presence of unloaded nanoparticles was investigated essentially as described by Dalpiaz et al. (2001b): the compounds were incubated at 37 °C in fresh whole blood obtained from healthy human volunteers. Blood was directly transferred to heparinised glass tubes. Three millilitres of whole blood were spiked with prodrug solutions or nanoparticle suspension resulting in final concentrations of 10 μM of Oct-CPA. If present, the concentration of unloaded nanoparticles was 3 mg/ml. During the experiment prodrug solutions were continuously gently shaken in an oscillating waterbath. At regular time intervals 100 μl of samples were taken, immediately hemolyzed in Eppendorf tubes prefilled with 500 μl of water (HPLC grade, 0 °C) and stored at −20 °C until analysis.

2.10. Oct-CPA kinetic analysis

Fifty microlitres of 10% sulphosalicilic acid were added to each sample together with 50 μl of internal standard (40 μM CH-CPA) and 200 μl of dichloromethane. The samples were extracted twice with 900 μl of water-saturated ethyl acetate. After 5 min of centrifugation at 9000 × *g*, the organic layer was evaporated to dryness by N_2 flow. The mobile phase (200 μl) was added and, after centrifugation, 20 μl were injected into the HPLC system and analysed as previously described.

2.11. Drug-receptor interaction studies

2.11.1. Cell culture

Cells were grown in 1:1 mixture of Dulbecco's modified Eagle's medium and Ham's F12 medium containing 10% foetal bovine serum (FBS), streptomycin (50 μg/ml) and penicillin (50 IU/ml) at 37 °C in 5% CO_2. Cells were subcultured twice weekly at a ratio of 1:10 and transferred to 14 cm diameter plates.

2.11.2. Membrane preparation

Cells were washed with phosphate buffered saline (PBS) and detached from plates by 5 min incubation at 37 °C in the presence of 2 ml of trypsol (0.25% trypsin, 4.4 mM EDTA in PBS). Five millilitres of medium were added to each plate after incubation, and the cells were collected and centrifuged for 10 min at 68 × *g*. Pellets derived from six plates were pooled and resuspended in 20 ml of ice-cold 50 mM Tris–HCl buffer, pH 7.4, and homogenised in a Polytron homogeniser (setting 6, model PT1200C, Brinkmann, Westbury, NY, USA) for 5 s. Plasma membranes and the cytosolic fraction were separated by centrifugation at 18,000 × *g* in a superspeed refrigerated centrifuge (model RC-5B, Sorvall, Wilmingtom, DE, USA) at 10 °C for 30 min. The pellets were resuspended in the Tris–HCl buffer at approximately 1×10^8 cells/3 ml and 2 IU/ml of ADA were added. After 30 min incubation at 37 °C, the membranes were stored in 200 μl aliquots at −80 °C. Membrane protein concentrations were measured with the bicinchoninic acid method (Smith et al., 1985).

2.11.3. Receptor binding assays

Membrane aliquots containing 40 μg of proteins were incubated in 400 μl of 50 mM Tris–HCl, pH 7.4, at 25 °C for 90 min, according to previous time course experiments. Saturation experiments were carried out using 12 different concentrations of [^{3}H]DPCPX ranging from 0.1 to 5 nM. Displacement experiments were performed using at least 20 different concentrations of cold drug in the presence of 1 nM [^{3}H]DPCPX. Non-specific binding was measured using 10 μM CHA. Separation of bound from free radioligand was performed by rapid filtration through GF/B filters (Whatman, Springfield Mill, UK), which were washed three times with ice-cold buffer. Filter bound

radioactivity was measured by scintillation spectrometry after adding of 4 ml Packard Emulsifier Safe (Packard Bioscience, Pero, Milan, Italy). All experiments were performed in the absence and in the presence of 50 μg/ml unloaded nanoparticles. All the values obtained are the means of three independent experiments performed in duplicate.

2.12. Calculations

2.12.1. Kinetics degradation in whole blood

The half life of Oct-CPA was calculated from an exponential decay plot of the peak area ratio between the compound and internal standard, expressed as percentage, versus incubation time, using the computer program GraphPad Prism (GraphPad, San Diego, CA, USA).

2.12.2. Binding assays

Data of saturation experiments (K_D and B_{max} values) were obtained by computer analysis of saturation curves and of the corresponding Scatchard plots. The cold drug concentrations displacing 50% of labelled ligand (IC_{50} values) were obtained by computer analysis of displacement curves. Inhibitory binding constants (K_i values) were derived from the IC_{50} values according to the Cheng and Prusoff equation $K_i = IC_{50}/(1 + [C^*]/K_D{}^*)$, where $[C^*]$ is the concentration of the radioligand and $K_D{}^*$ its dissociation constant (Cheng and Prusoff, 1973). Care was taken to ensure total binding never exceeded 10% of the total amount of radioligand added.

2.12.3. Statistical analysis

One way ANOVA followed by Dunnett's t test was performed using the computer program GraphPad Prism (GraphPad). Difference was considered statistically significant at P values less than 0.05.

3. Results

3.1. The effect of both the surfactants and the recovery methods on nanoparticle properties

Table 1 shows the recovery percentage, the drug content and the entrapment efficiency of the Oct-CPA loaded nanoparticles as function of both the surfactants and the recovery methods. The sample prepared using sodium cholate and recovered by ultra-centrifugation is not reported because it resulted in a not redispersible cake.

Regardless of the surfactants, the recovery of the nanoparticles was quantitative only for the samples purified by dialysis (samples A and C); however, for the others samples the recovery percentage was acceptable, ranging between 60 and 75%. Moreover, a residual of stabilizing agent was found in all the samples of dried nanoparticles. In particular, as reported in Table 1, this residual was higher for the samples purified by dialysis (A and C; about 20%) with respect to the samples recovered by the gel-filtration or ultra-centrifugation techniques (B, D and E; from 0.5 to 5.2%).

As for prodrug contents, the formulations A and B were obtained using sodium cholate and displayed higher Oct-CPA amounts (1.30 and 0.38% (w/w), respectively) than the corresponding formulations obtained in the presence of Pluronic (C and D; 0.63 and 0.13% (w/w), respectively). On the other hand, both the prodrug content and encapsulation efficiency were higher for the samples purified by dialysis (A and C) rather than by gel-filtration (B and D), independently on the surfactant used in the formulations. Finally, the sample E, prepared in presence of Pluronic and recovered by ultra-centrifugation, displayed satisfactory both drug content and encapsulation efficiency (1.13 ± 0.1% (w/w) and $42.3\% \pm 2.8$, respectively).

3.2. Size and morphology of nanoparticles

Fig. 2 reports the particles size distribution (PSD) elaborated from SdFFF fractograms, assuming the density of all nanoparticle samples to be 1.4 g/ml. This value, indeed, allowed the peaks of PSD plots to correspond to the size of nanoparticles obtained by electronic microscopy analysis. The patterns reported in Fig. 2 have been obtained with samples usually sonicated for 10 min before the injection in the SdFFF channel.

Graphs referred to samples A and B both present an initial narrow and well distinguished peak, their maxima were evaluated, according to the procedure process, to be, respectively, at 91 (±4) and 80 (±7) nm. From their shape, it can be deduced that they have been likely generated by a quite narrow size population of particles. The shape of the signal profile between 0.2 and 0.4 μm was not reproducible, but dependent on the sample treatment before the injection in the SdFFF channel; in particular, it has been observed the appearance of more peaks when the sonication time was increased from 10 to 30 min (data not shown). Probably, the sonication process generates aggregates among particles, fostered also by the increase of the temperature, which occurs during the process.

Table 1
The effect of both the surfactants and the purification method on the recovery percentage, the residual of surfactants, prodrug loading and entrapment efficiency of the Oct-CPA loaded nanoparticles

Sample	Surfactant	Purification method	Recovery (%)	Residual of surfactant (%, w/w)	Oct-CPA loading (%, w/w ± S.D.)	Entrapment efficiency (% ± S.D.)
A	Sodium cholate	Dialysis	100	20.0 ± 3.0	1.30 ± 0.08	65.0 ± 3.1
B	Sodium cholate	Gel-filtration	60	5.2 ± 1.8	0.38 ± 0.03	11.4 ± 2.2
C	Pluronic F68	Dialysis	100	21 ± 2.2	0.63 ± 0.06	31.5 ± 1.7
D	Pluronic F68	Gel-filtration	70	0.5 ± 0.2	0.13 ± 0.02	4.5 ± 0.5
E	Pluronic F68	Ultra-centrifugation	75	0.9 ± 0.3	1.13 ± 0.10	42.3 ± 2.8

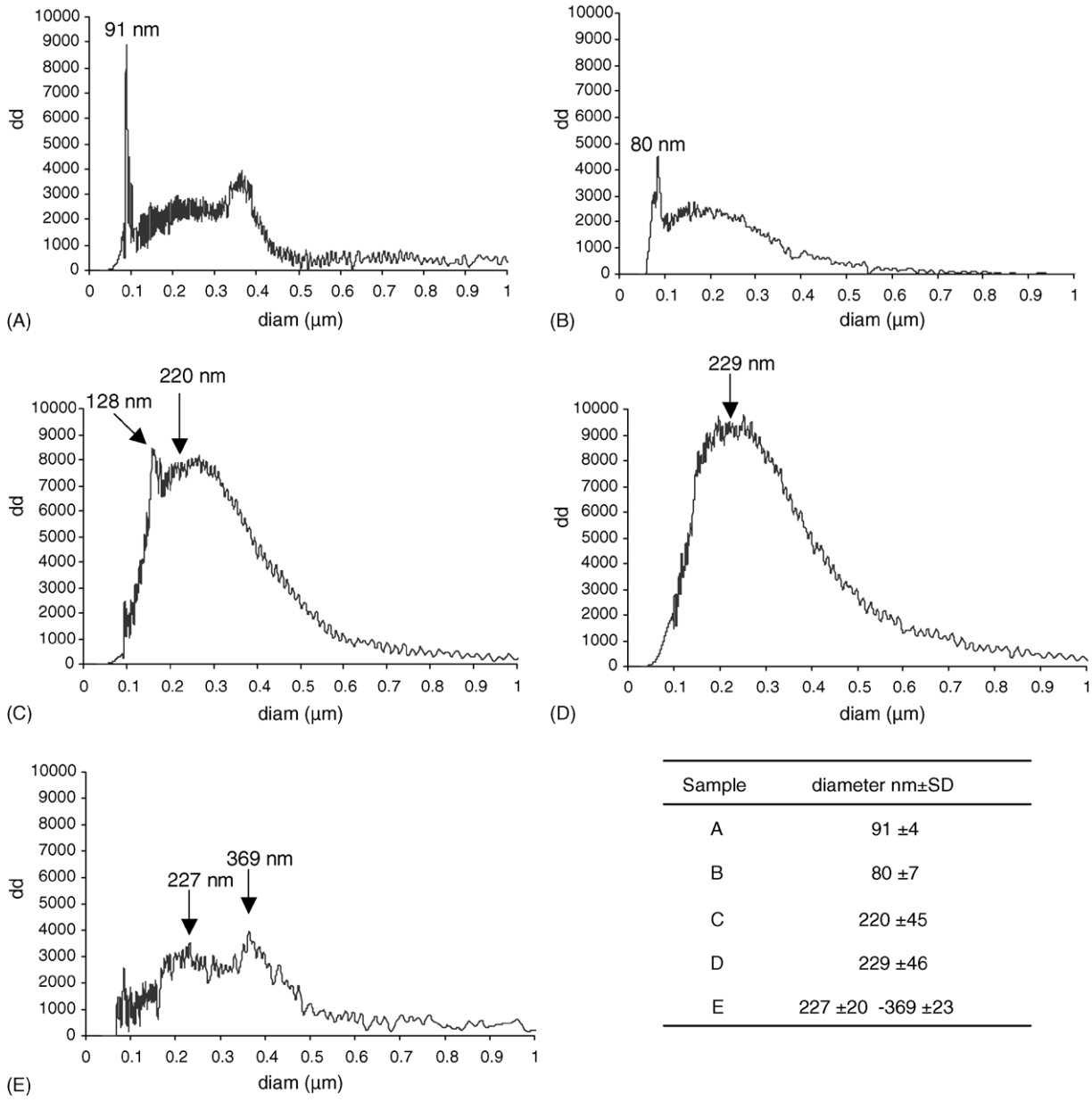

Sample	diameter nm±SD
A	91 ±4
B	80 ±7
C	220 ±45
D	229 ±46
E	227 ±20 -369 ±23

Fig. 2. PSD elaborated from SdFFF fractograms obtained under power programmed elution conditions: sample A (initial field = 1200 rpm, relaxation time 15 min, t_1 = 8 min, t_a = −64 min, final field = 20 rpm), samples B, C, D, E (initial field = 1000 rpm, relaxation time 10 min, t_1 = 5 min, t_a = −40 min, final field = 20 rpm). Particles were assumed to have a density of 1.4 g/ml (diam = diameter of nanoparticles; dd = dimensional distribution). The table reports the mean diameter and the related standard deviation of nanoparticles obtained by the deconvolution procedure of PSD.

The particle size distribution profiles reported in graphs referred to samples C and D show a more regular shape in comparison with the previous two; indeed, for both it can be identified a major, broad and tailed peak, whose maxima were evaluated to be, respectively, at 220 (±45) and 229 (±46) nm; in addition graph C present also a small peak at about 128 (±10) nm. The presence of a main mono-modal distribution cannot, however, be assigned to the presence of a single particle population, since also in this case, the sonication treatment could have produced particle aggregates, whose presence contributes to tailing the peaks.

The injection of sample E generated a fractogram which allows to identify the presence of two peaks evaluated mainly at 227 (±20) and 369 (±23) nm, whom corresponds the bi-modal particle size distribution reported on graph E. Its pattern shows a base line quite noisy also at high retention times, indicating an high probability to find nanoparticles of size greater than 500 nm, in the injected suspension. This analysis of graph E is supported by the evidence that the sonication time does not change the shape of the elution profile, as occurred, instead, for sample A.

Representative results of the analysis on nanoparticles morphology using scanning electron microscopy are shown in Fig. 3. The sample B prepared using sodium cholate (Fig. 3a) appeared spherical in shape although no details in the surface morphology were observable owing to the small particle size. Nanoparticle

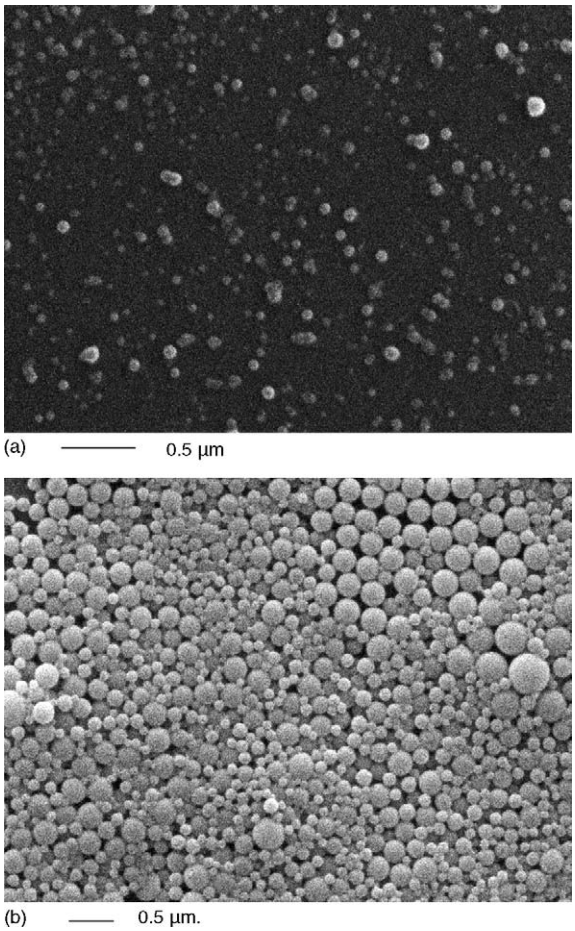

Fig. 3. Scanning electron micrograph of Oct-CPA nanoparticles prepared using sodium cholate (a), magnification: ×25,000, sample B; Pluronic F68 (b), magnification: ×10,000, sample D.

surface was observed only for the larger particles prepared in presence of Pluronic. As an example, we reported the SEM analysis of the sample D (Fig. 3b), for which a spherical shape with a smooth surface was observed.

3.3. In vitro release study

The release profiles of Oct-CPA loaded nanoparticles showed a bi-phasic pattern for all the samples taken into account (Fig. 4).

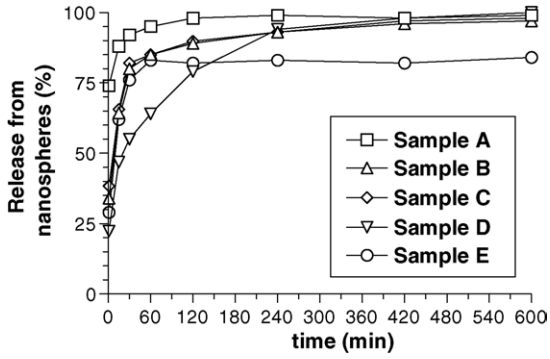

Fig. 4. In vitro release of Oct-CPA from poly(lactic acid) nanoparticles obtained in 20 ml of 0.1 phosphate buffer at 37 °C. Results are the means of three independent experiments performed in duplicate (S.D. less than 10%).

The rate in the first release phase (burst effect) may be evaluated according to the T_d value reported in Table 2. This value indicates the time period during which the 62.5% of the encapsulated drug was released (Langenbucher, 1972). The most quickly drug release was observed for sample A ($T_d = 0.4 \pm 0.1$ min), corresponding to the smallest nanoparticles prepared using sodium cholate and recovered by dialysis. It is to underline that the sample A showed a release profile practically identical to the dissolution profiles obtained from the free prodrug in presence of Pluronic or sodium cholate (data not shown). On the other hand, a significant decrease of the release rate was obtained by recovering the Oct-CPA loaded nanoparticles by gel-filtration. In fact, the prodrug was released from sample B ($T_d = 10 \pm 1$ min) with a lower rate than sample A. The samples C ($T_d = 9 \pm 4$ min) and D ($T_d = 37 \pm 5$ min), prepared in the presence of Pluronic, showed not only a similar dependence on the recovery method, but also a release rate lower than their homologues obtained using sodium cholate (samples A and B, respectively). In particular, the sample D showed the most slow burst effect among the nanoparticles taken into account. The slowest rate of the prodrug delivery during the second release phase was showed, instead, by sample E, which was obtained in the presence of Pluronic and recovered by gel-filtration.

3.4. Stability of Oct-CPA in human whole blood

Free Oct-CPA was hydrolyzed in human whole blood following a first order kinetic (Fig. 5) whose half life was 31 ± 3 min

Table 2
Half life values referred to the release of encapsulated Oct-CPA in phosphate buffer from nanoparticles and its hydrolysis in human whole blood in comparison to free Oct-CPA

Sample	Oct-CPA Release T_d (min ± S.D.)	Oct-CPA half life in blood (min ± S.D.)	Free Oct-CPA half life in blood-presence of unloaded nanoparticles (min ± S.D.)
A	0.4 ± 0.1	30 ± 2	31 ± 3
B	10 ± 1	59 ± 5[a]	32 ± 3
C	9 ± 4	51 ± 4[b]	29 ± 2
D	37 ± 5	88 ± 5[a]	31 ± 3
E	14 ± 3	31 ± 3[c]	30 ± 2

The half life value of free Oct-CPA alone in human whole blood is 30 ± 3 min.
[a] $P < 0.001$, significantly different from the half life value of free CPA alone.
[b] $P < 0.05$, significantly different from the half life value of free CPA alone.
[c] Half life value referred to the hydrolysis pattern choosing the bottom plateau at about 20% (see Fig. 5).

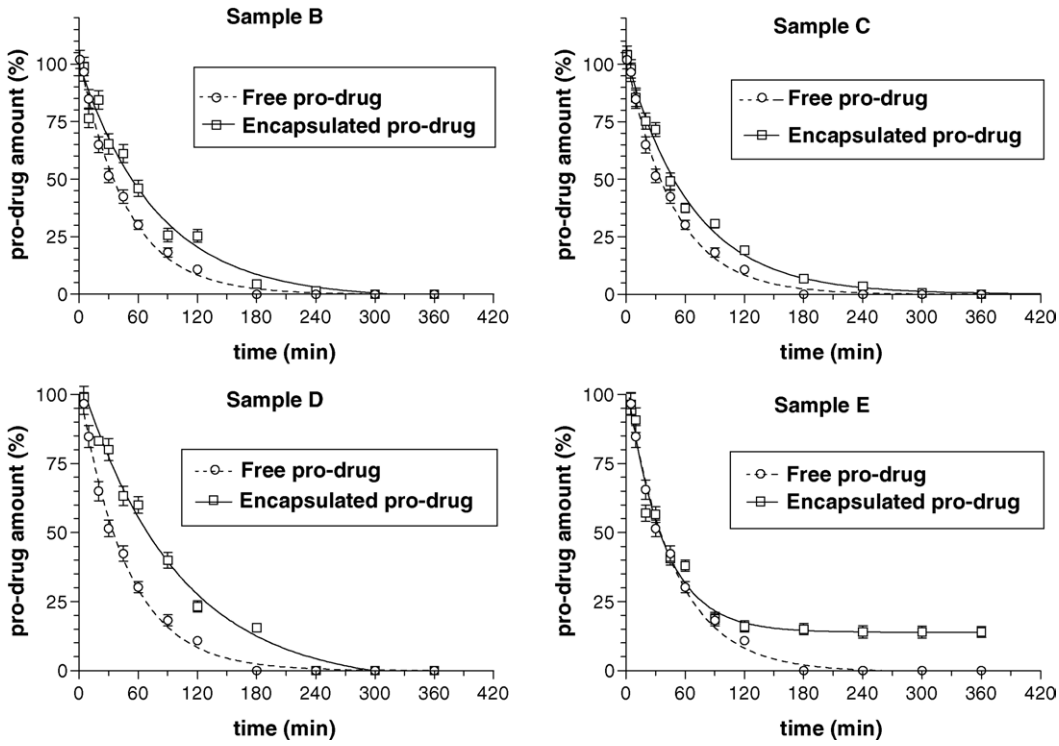

Fig. 5. Degradation kinetics in human whole blood of free or encapsulated Oct-CPA in different samples of nanoparticles. The plots show the percentage of the total prodrug amount vs. time, obtained from the peak area ratio between the compound and its internal standard. Results are the means of three independent experiments performed in duplicate (standard errors are reported).

(Table 2). This pattern was not significantly modified in the presence of unloaded samples A–E of nanoparticles and a similar result was obtained for the prodrug encapsulated in the sample A (data not shown). On the other hand, the whole blood degradation of Oct-CPA encapsulated in the other nanoparticle samples (B, C, D, E) appeared significantly slower with respect to the free prodrug (Fig. 5). In particular, the half life values of Oct-CPA degradation increased from 31 ± 3 to 59 ± 5 min for sample B, 51 ± 4 min for sample C and 88 ± 5 min for sample D (Table 2). Finally, the sample E did not show any influence toward hydrolysis rate of about the 80% of encapsulated prodrug (half life = 31 ± 3 min, Table 2), whereas it appeared to induce a strong stability to the remaining 20%.

3.5. Receptor binding assays

CPA shows high affinity toward adenosine A_1 receptor, with respect to Oct-CPA (Dalpiaz et al., 2001a). As a consequence, a potential activation of the A_1 receptor cannot be induced by the prodrug released from the nanoparticles: only the CPA delivered by Oct-CPA hydrolysis can activate the receptor. In the aim to verify if the presence of the controlled release systems may interfere with the CPA-receptor interaction, we have performed receptor binding experiments in vitro both in the absence and in the presence of unloaded nanoparticles of samples A–E. The A_1 affinity of CPA has been obtained by investigating its ability to compete with [^{3}H]DPCPX, a radiolabeled antagonist. Table 3

Table 3
Equilibrium binding parameters obtained for [^{3}H]DPCPX and CPA in the absence and in the presence of different samples (50 μg/ml) of unloaded nanoparticles

Ligand	Nanoparticle absent	Unloaded sample A	Unloaded sample B	Unloaded sample C	Unloaded sample D	Unloaded sample E
[^{3}H]DPCPX						
K_D (nM)	1.53 ± 0.07	1.54 ± 0.07	1.60 ± 0.07	1.62 ± 0.08	1.57 ± 0.07	1.63 ± 0.08
B_{max}[a]	998 ± 14	996 ± 13	993 ± 14	983 ± 12	976 ± 12	991 ± 13
CPA						
$K_{i,high}$ (nM)	3.2 ± 0.2	3.4 ± 0.4	3.2 ± 0.3	3.3 ± 0.3	3.0 ± 0.2	3.1 ± 0.3
$K_{i,low}$ (nM)	74 ± 6	73 ± 6	76 ± 6	72 ± 5	77 ± 5	75 ± 6
f high	0.71 ± 0.03	0.71 ± 0.03	0.74 ± 0.04	0.72 ± 0.04	0.69 ± 0.02	0.73 ± 0.04

The parameters are expressed as (1) dissociation constants, K_D and B_{max} (for [^{3}H]DPCPX) derived from saturation experiments; (2) inhibitory constants, K_i and fraction of receptor high affinity state, *f* high (for CPA) derived from inhibition experiments.

[a] fmol/mg protein.

reports the K_D and B_{max} values obtained by saturation experiments referred to [^{3}H]DPCPX: in the absence of nanoparticles the values were 1.53 ± 0.07 nM and 998 ± 14 fmol/mg protein, respectively, as previously found by us in the same experimental system (Dalpiaz et al., 1998, 2001b, 2002). These values were not significantly changed in the presence of unloaded nanoparticles. As for CPA, the K_i values reported in Table 3 indicate that in absence of nanoparticles this ligand recognised two affinity binding states ($K_{i,high} = 3.2 \pm 0.2$ nM; $K_{i,low} = 74 \pm 6$ nM) with about 70% of high affinity population. All binding data referred to CPA were not significantly changed in the presence of unloaded samples, as shown in Table 3. These results suggest, therefore, that the ligand binding to adenosine A_1 receptor is not altered by the presence of the controlled release systems.

4. Discussion

The lipophilic properties of Oct-CPA (log $P = 3.91$, Dalpiaz et al., 2001a) induce this prodrug to have a relatively poor solubility in water with respect to a good solubility in organic solvents, such as DMSO and methanol. Because of the prodrug was hydrophobic, poly(D,L lactic acid) rather than (poly D,L lactide-co-glicolide) was chosen as polymer. Moreover, nanoprecipitation procedure was therefore considered an appropriate method in order to retain Oct-CPA in the hydrophobic nanoparticle matrix.

Two different organic solvents were used in the nanoparticle preparation: acetone for the polymer and methanol for the prodrug. This choice was adopted because the prodrug appeared poorly soluble in the main solvents generally used to dissolve the polymer. For this reason, the simultaneous precipitation of prodrug and polymer was not accomplished obtaining, thus, an incomplete entrapment of the prodrug in the nanoparticle matrix. In order to recover the nanoparticles without both the unencapsulated prodrug and the excess of surfactants, dialysis, gel-filtration or ultra-centifugation techniques were employed before freeze-drying the samples.

The results reported in Table 1 indicate that Oct-CPA entrapment into the nanoparticles was dependent on the recovery method. Even if the dialysis method appeared excellent in terms of the recovery percentage, the T_d values reported in Table 2 indicate an higher burst effect for nanoparticles recovered by dialysis (samples A and C) with respect to the homologues recovered by gel-filtration (samples B and D, respectively), suggesting, therefore, a greater presence of adsorbed prodrug on the surface of dialyzed samples. These data indicate, therefore, the gel-filtration as a preferable recovery method of the loaded nanoparticles, with respect to dialysis, despite this last process can be related to excellent recovery values of the prodrug.

Oct-CPA entrapment into the nanoparticles did not significantly affect particle size; in fact, any direct correlation was obtained between Oct-CPA content and nanoparticle size. On the other hand, nanoparticle size appeared strongly influenced from both the surfactant and the recovery method used in the nanoparticle preparation (see Fig. 2). As concern the influence of the surfactant, samples prepared in presence of sodium cholate (A and B) resulted remarkably smaller with respect to the samples prepared in presence of Pluronic (C–E). These results well agree with those reported in literature indicating effectiveness in reducing the size and the size range of nanoparticles using sodium cholate in the nanoparticle preparation (Gref et al., 1995; Panagi et al., 2001).

The size of the Oct-CPA loaded nanoparticles (which was strongly dependent on the surfactant choice), as well as the recovery method significantly affected the prodrug release rate. In particular, a comparison between the samples obtained in the presence of sodium cholate (A and B) with the homologues obtained in the presence of pluronic (C and D, respectively), indicates that samples recovered by gel-filtration released the prodrug more slowly than those purified by dialysis (Table 2). In particular, the lower burst effects observed for the corresponding samples purified by gel-filtration suggest this recovery method very efficient in the removal of the unentrapped prodrug. It is to underline that sample D (obtained in the presence of Pluronic and recovered by gel-filtration) displayed not only the lowest burst effect, among the nanoparticles obtained, but also a delayed release during the second release phase, probably ascribed to the deeply entrapped drug. Hence, this sample seemed to provide an acceptable control of the prodrug release.

Finally, the prodrug release from the sample E, obtained in the presence of Pluronic and recovered by ultra-centrifugation was characterised by a large burst effect attributable to the unentrapped prodrug that remains associated to nanoparticles during the ultra-centrifugation process. Indeed, this procedure allowed an efficient removal of the water-soluble compounds as surfactant but not of the water-insoluble compound as the prodrug. For this sample the second phase of the prodrug release pattern, generally attributable to the drug entrapped in the core of the nanoparticles, was very slow. This excellent control of the prodrug delivery may be attributable to the presence of larger sized nanoparticles and/or aggregates as highlighted by the SdFFF fractograms.

According to the release profiles, Oct-CPA showed different degree of stabilization in human whole blood, in dependence on the samples of nanoparticles where it was encapsulated. In particular, the smallest nanoparticles purified by dialysis (Sample A) did not allow to increase the Oct-CPA stability in human whole blood. A significant stabilization was obtained, instead, in the case of the corresponding nanoparticles purified by gel-filtration (Sample B), which allowed to double the prodrug half life in human whole blood. Interestingly, a similar result was also obtained using the larger nanoparticles (i.e. obtained in the presence of Pluronic) purified by dialysis (Sample C). It is to underline that the same nanoparticles obtained in the presence of Pluronic, but recovered by gel-filtration (Sample D) allowed to increase the Oct-CPA half life in whole blood up to three times with respect to the free prodrug. Moreover, the sample recovered by ultra-centrifugation (Sample E), allowed to strongly stabilise about the 20% of Oct-CPA. These results indicate the choose of recovery method of nanoparticles as a way to sensibly modulate the release and related increase of stability in physiological fluids of the encapsulated prodrug. The slowest prodrug releases from the nanoparticles should allow to obtain, in vivo, a reduction of the side effects induced by CPA. Indeed, the small amounts of

free drug delivered after the prodrug hydrolysis, should occupy a small amount of receptors during the first times of Oct-CPA release, as previously found for CPA released from microparticles (Dalpiaz et al., 2001b). The amounts of free CPA may increase during time, with a pattern related to the release from nanoparticles of the prodrug (Dalpiaz et al., 2001b) and its subsequent hydrolysis (Dalpiaz et al., 2001a), but the relatively fast degradation of CPA in vivo should maintain poor its concentration in the blood.

We have previously demonstrated that Oct-CPA shows a poor affinity toward adenosine A_1 receptor with respect to CPA, which can be obtained by the prodrug hydrolysis (Dalpiaz et al., 2001a). In the aim to verify if the controlled release systems can interfere with CPA interaction toward adenosine A_1 receptor, we have performed the receptor binding experiments whose results are reported in Table 3. Our results indicate that all the nanoparticle samples investigated do not contribute to change the affinity of CPA for the high and low affinity states of the adenosine A_1 receptor. We can, therefore, conclude that the unloaded nanoparticles of samples A–E do not interfere with the interaction of CPA toward adenosine A_1 receptor, independently on the surfactants and recovery methods adopted for their preparation.

Acknowledgements

This research was supported by Italian Ministry of University, Scientific and Technological Research (MURST). The authors thank Prof. Peter R. Schofield of the Garvan Institute of Medical Research, Sydney, Australia and Dr. Andrea Townsend-Nicholson of the Department of Anatomy and Developmental Biology, University College, London, for providing CHO A_1 cells. Moreover, the authors thank the Laboratorio Analisi Estense of Ferrara, Italy, for supplying fresh blood.

References

Bischofberger, N., Jacobson, K.A., von Lubitz, D.K., 1997. Adenosine A_1 receptor agonists as clinically viable agents for treatment of ischemic brain disorders. Ann. N.Y. Acad. Sci. 825, 23–29.

Brodie, M.S., Lee, K., Fredholm, B.B., Stahle, L., Dunwiddie, T.V., 1987. Central nervous peripheral mediation of responses to adenosine receptor agonists: evidence against a central mode of action. Brain Res. 415, 323–330.

Caldwell, K.D., Li, J.M., 1989. Emulsion characterization by the combined sedimentation field-flow fractionation–photon correlation spectroscopy methods. J. Colloid Interface Sci. 132, 256–268.

Calvo, P., Gouritin, H., Villarroya, B., Eclancher, F., Giannavola, C., Klein, C., Andreux, J.P., Couvreur, P., 2002. Quantification and localization of PEGylated polycyanoacrylate nanoparticles in brain and spinal cord during experimental allergic encephalomyelitis in the rats. Eur. J. Neurosci. 15, 1317–1326.

Cheng, Y.C., Prusoff, W.H., 1973. Relationships between the inhibition constant (K_i) and the concentration of inhibitor which cause 50 per cent inhibition (IC_{50}) of an enzymatic reaction. Biochem. Pharmacol. 22, 3099–3108.

Childs, C.E., 1975. Determination of polyoxyethylen glycol in gammaglobulin solutions. Microchem. J. 20, 190–192.

Contado, C., Blo, G., Fagioli, F., Dondi, F., Beckett, R., 1997. Characterisation of river Po particles by SdFFF-ICP-MS and AAS. Colloid. Surf. A 120, 47–59.

Dalpiaz, A., Manfredini, S., 2002. Adenosine A_1 receptors: analysis of the potential therapeutic effects obtained by its activation in the central nervous system. Curr. Med. Chem. 9, 1923–1937.

Dalpiaz, A., Scatturin, A., Menegatti, E., Bortolotti, F., Pavan, B., Biondi, C., Durini, E., Manfredini, S., 2001a. Synthesis and study of 5′-ester prodrugs of N^6-cyclopentyladenosine, a selective A1 receptor agonist. Pharm. Res. 18, 531–536.

Dalpiaz, A., Scatturin, A., Pavan, B., Biondi, C., Vandelli, M.A., Forni, F., 2001b. Poly(lactic acid) microspheres for the sustained release of a selective A_1 receptor agonist. J. Control. Release 73, 303–313.

Dalpiaz, A., Scatturin, A., Pavan, B., Biondi, C., Vandelli, M.A., Forni, F., 2002. Poly(lactic acid) microspheres for the sustained release of antiischemic agents. Int. J. Pharm. 242, 115–120.

Dalpiaz, A., Townsend-Nicholson, A., Beukers, M.W., Schofield, P.R., IJzerman, A.P., 1998. Thermodynamics of full agonist, partial agonist and antagonist binding to wild type and mutant adenosine A_1 receptors. Biochem. Pharmacol. 56, 1437–1445.

Dalpiaz, A., Leo, E., Vitali, F., Pavan, B., Scatturin, A., Bortolotti, F., Manfredini, S., Durini, E., Forni, F., Brina, B., Randelli, M.A., 2005. Development and characterization of biodegradable nanospheres as delivery systems of anti-ischemic adenosine derivatives. Biomaterials 26, 1299–1306.

de Mendonca, A., Sebastiao, A.M., Ribeiro, J.A., 2000. Adenosine: does it have a neuroprotective role after all? Brain Res. Rev. 33, 258–274.

Fessi, H., Puisieux, F., Devissaguet, J.P., Ammoury, N., Benita, S., 1989. Nanocapsule formation by interfacial polymer deposition following solvent displacement. Int. J. Pharm. 55, R1–R4.

Fredholm, B.B., Abbracchio, M.P., Burnstock, G., Daly, J.W., Harden, T.K., Jacobson, K.A., Leff, P., Wlliams, M., 1994. Nomenclature and classification of purinoceptors. Pharmacol. Rev. 46, 143–156.

Giddings, J.C., 1993. Field-flow fractionation: separation and characterization of macromolecular–colloidal–particulate materials. Science 260, 1456–1465.

Giddings, J.C., 1995. Measuring colloidal and macromolecular properties by FFF. Anal. Chem. 67, 592A–598A.

Giddings, J.C., Ho, J., 1995. Accurate measurement of density of colloidal latex particles by sedimentation field-flow fractionation. Langmuir 11, 2399–2404.

Giddings, J.C., Williarns, P.S., 1993. Multifaceted analysis of 0.01 to 100 um particles by sedimentation field-flow fractionation. Am. Lab. 95, 88–95.

Gref, R., Domb, A., Quellec, P., Blunk, T., Muller, R.H., Verbavats, J.M., Langer, R., 1995. The controlled intravenous delivery of drugs using PEG-coated sterically stabilized nanospheres. Adv. Drug Deliv. Rev. 16, 215–223.

Jacobson, K.A., Trivedi, B.K., Churchill, P.C., Williams, M., 1991. Novel therapeutics acting via purine receptors. Biochem. Pharmacol. 41, 1399–1410.

Johansson, B., Halldner, L., Dunwiddie, T.V., Masino, S.A., Poelchen, W., Gimenez-Llort, L., Escorihuela, R.M., Fernandez-Teruel, A., Wiesenfeld-Hallin, Z., Xu, X.J., Hardemark, A., Betsholtz, C., Herlenius, E., Fredholm, B.B., 2001. Hyperalgesia, anxiety, and decreased hypoxic neuroprotection in mice lacking the adenosine A_1 receptor. Proc. Natl. Acad. Sci. U.S.A. 98, 9407–9412.

Kirkland, J.J., Yau, W.W., Doerner, W.A., 1980. SdFFF of macromolecules and colloids. Anal. Chem. 52, 1944–1954.

Kreuter, J., Petrov, V.E., Kharkevich, D.A., Alayautdin, R.N., 1997. Influence of the type of surfactant on the analgesic effects induced by the peptide dalargin after 1st delivery across the blood-brain barrier using surfactant coaded nanoparticles. J. Control. Release 49, 81–87.

Langenbucher, F., 1972. Linearization of dissolution rate curves by Weibull distribution. J. Pharm. Pharmacol. 24, 979–981.

Mathot, R.A., van Schaick, E.A., Langemeijer, M.W., Soudijn, W., Breimer, D.D., IJzerman, A.P., Danhof, M., 1994. Pharmacokinetic-pharmacodynamic relationship of the cardiovascular effects of adenosine A1 receptor agonist N^6-cyclopentyladenosine in the rat. J. Pharmacol. Exp. Ther. 268, 616–624.

Mucci, A., Schenetti, L., Salvioli, G., Ventura, P., Vandelli, M.A., Forni, F., 1996. The interaction of biliar acid with 2-hydroxypropyl-b-

cyclodextrn in solution and in solid state. J. Incl. Phenom. 26, 233–241.

Muller, C.E., 2000. Adenosine receptor ligands—recent developments. Part I. Agonists. Curr. Med. Chem. 7, 1269–1288.

Panagi, Z., Beletsi, A., Evangelatos, G., Livaniou, E., Ethakissios, D.S., Avgoustakis, K., 2001. Effect of dose on the biodistribution and phamacokinetics of PLGA and PLGA-mPEG nanoparticles. Int. J. Pharm. 221, 143–152.

Pavan, B., IJzerman, A.P., 1998. Processing of adenosine receptor agonists in rat and human whole blood. Biochem. Pharmacol. 56, 1625–1632.

Ralevic, V., Burnstock, G., 1998. Receptors for purines and pyrimidines. Pharmacol. Rev. 50, 413–492.

Smith, P.K., Krohn, R.I., Hermanson, G.T., Mallia, A.K., Gartner, F.H., Provenzano, M.D., Fujimoto, E.K., Goeke, N.M., Olson, B.J., Klenk, D.C., 1985. Measurement of protein using bicinchoninic acid. Anal. Biochem. 150, 76–85.

Townsend-Nicholson, A., Schofield, P.R., 1994. A threonine residue in the seventh transmembrane domain of the human A_1 adenosine receptor mediates specific agonist binding. J. Biol. Chem. 269, 2373–2376.

Townsend-Nicholson, A., Shine, J., 1992. Molecular cloning and characterisation of a human brain A_1 adenosine receptor cDNA. Brain Res. Mol. Brain Res. 16, 365–370.

Von Lubitz, D.K., Marangos, P.J., 1990. Cerebral ischemia in gerbils: postischemic administration of cyclohexyladenosine and 8-sulfophenyltheophylline. J. Mol. Neurosci. 2, 53–59.

Von Lubitz, D.K., Lin, R.C., Bischofberger, N., Beenhakker, M., Boyd, M., Lipartowska, R., Jacobson, K.A., 1999. Protection against ischemic damage by adenosine amine congener, a potent and selective adenosine A_1 receptor agonist. Eur. J. Pharmacol. 369, 313–317.